ELSEVIER

Journal of Power Sources 90 (2000) 125–134

JOURNAL OF POWER SOURCES

www.elsevier.com/locate/jpowsour

Effect of Na_2SO_4 additive in positive electrodes on the performance of sealed lead-acid cells for electric scooter applications

Jenn-Shing Chen *

Department of Chemical Engineering, I-Shou University, Ha-Hsu Hsiang, Kaohsiung 84008, Taiwan

Received 25 May 1999; accepted 17 June 1999

Abstract

This study investigated the effects of Na_2SO_4 additive in the positive electrode on the performance of sealed lead-acid cells. The additive Na_2SO_4 in the cured plates can reduce the 4BS crystal size, which produces a smaller α-PbO_2 and β-PbO_2 crystal size in the formed plates, which will have a larger surface area. The plate's chemical composition is independent of the amount of Na_2SO_4 additive in the positive electrodes. Plate composition relies only on the cure temperature conditions. Increasing amounts of Na_2SO_4 additive to the positive electrode will not decrease the crystal size appreciably. The optimal amount of Na_2SO_4 additive is 0.01–0.05 M, which produces the smallest crystal size and largest specific surface area. Cells with Na_2SO_4 additive in the positive plates have a smaller surface area, causing a higher initial capacity and average capacity per cycle for both testing methods: the standard cycle testing and the electric scooter (ES) driving pattern cycle testing. The initial capacity and average capacity can be increased up to 4% in the standard cycle testing and up to 8% in the ES driving pattern cycle testing.

Keywords: Sealed lead-acid cell; Electric scooters; Positive plates; Additives; Curing temperature

1. Introduction

Electric scooters (ESs) have recently come into commercial use. However, the lower traveling range and higher initial cost give ESs lower performance than internal combustion (IC) scooters which are not attractive to consumers. Increasing the storage capacity and power output of ES batteries will increase an ES's range. Generally, the higher the energy density, the lower battery the application costs. The battery cost is critical to the total ES cost. The battery cost is 30–35% of the entire ES price. Therefore, the battery selected for ES applications is critical toward improving ES performance. Two types of batteries are quite attractive and feasible for ES applications in the commercial battery market: the valve-regulated lead-acid (VRLA) battery (Pb/PbO_2) and the nickel/metal-hydrate battery (Ni/MH). Although the Ni/MH performance is better than that of Pb/PbO_2, Ni/MH is economically unattractive for ES commercialization. The cost of a Ni/MH battery alone rivals the cost of the entire IC motorcycle. For this reason, VRLA batteries are used in commercial ES. The general advantages of VRLA batteries are low cost, free maintenance, high reliability, high discharge rate capability, and low self-discharge rate. However, the principal disadvantages, low energy density and short cycle life, have limited the use of this battery to ES applications. Increasing the energy density and improving the cycle life are key technology improvements for VRLA batteries in ES applications.

In our earlier paper [1], we investigated how the curing temperature affects the composition and material structure of the positive plate in ES lead-acid cells. According to the experimental results, the major morphology in positive active-material crystals is tribasic lead sulfate (= 3BS) at low temperatures and tetrabasic lead sulfate (= 4BS) at high curing temperatures (> 65°C). The 4BS and α-PbO_2 crystals are larger than the 3BS and β-PbO_2 crystals; hence, the pore surface area is small. After plate formation, 4BS favors the formation of α-PbO_2, and 3BS yields β-PbO_2 phase. The formation of 3BS-rich plates apparently leads to a higher β-PbO_2 content than 4BS-rich plates. The results show that higher temperature cured plates have less initial capacity but longer cycle life, as revealed by the ES driving pattern cycle testing. Also, many papers [2–5] have shown that higher cure temperature forms 4BS-rich positive plate materials, which have

* Tel.: +886-7-656-3711; fax: +886-7-656-3734

0378-7753/00/$ - see front matter
PII: S0378-7753(99)00308-0

stronger mechanical strength and enhance the cycle life for deep-discharge applications in sealed lead-acid batteries. This study is a continuation of our previous studies to develop a high-performance VRLA cell particularly for increasing the specific energy and cycle life for ES applications. Higher temperature cured positive plates were used in this work in order to enhance the VRLA battery service life for ES applications. Additives to the positive electrode were used to increase the capacity. In the VRLA cells, the utilization of active materials remained very low (about 30% at the 1 C rate) for the positive plate, while strenuous efforts were made to increase additives to the plate active materials [6]. Many materials have been proposed as additives for the positive active mass [7–10]. The additive Na_2SO_4 in positive electrode material can reduce the 4BS size of electrode materials [10], leading to a large capacity. In this work, we studied the effect of Na_2SO_4 additive in the positive electrode on the performance of VRLA cells for ES applications.

2. Experimental procedures

2.1. Cell construction

Each cell contained two positive plates and three negative plates. The positive paste was prepared by mixing leady oxide with water, sulfuric acid, fiber and Na_2SO_4 additive. The paste compositions were 50 kg ball-mill leady oxide, 6000 cm^3 water, 3500 cm^3 sulfuric acid of 1.40 specific gravity, 50 g short fiber and in the presence of varying amounts of Na_2SO_4 from 0.01 to 2 M, according to the volume of sulfuric acid. Mixing was continued for 35 min and the paste's apparent density was about 4.1 g cm^{-3}. Next, the paste was applied to grids cast from a Pb/Ca alloy. The grid dimensions were 69 mm × 40 mm × 3.6 mm. The positive plates were controlled with around 33 g paste on both sides of each grid and then cured. Curing was performed for 1 day at 85°C at a relative humidity $>90\%$. Prior to electroformation, the plates were dried in the air for 3–5 days until the moisture in the paste was <1 wt.%. The current density was controlled at 6 mA cm^{-2} and the formation capacity had a theoretical capacity of about 200% under the formation. After formation, the plates were washed in running water for several hours and then dried in an oven at 65°C for 24 h. All negative plates and absorptive glass-mat (AGM) separators applied in this work were furnished by The Ztong Yee Battery (Taiwan). Each cell was filled with 38 cm^3 of electrolyte and then sealed with a cover. In all experiments, the electrolyte was a sulfuric acid solution having a specific gravity of 1.335 (20°C). The cell's rated capacity was 4 A h.

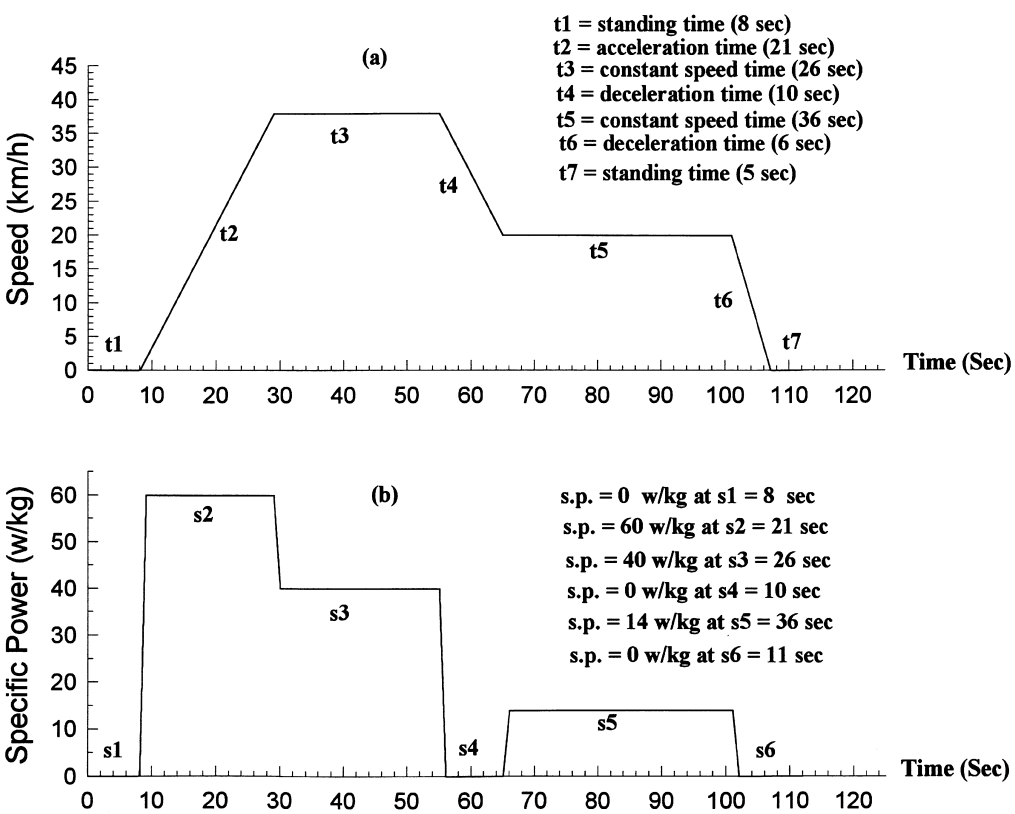

Fig. 1. (a) Velocity vs. time schedule for CNS-D3029 profile. (b) Battery power required by Improved Sanyang Dio Electric Scooter to negotiate the velocity schedule in (a).

2.2. Cell cycling tests

The cells were cycled under computer-controlled charge and discharge regimens using the Arbin Battery Testing System. To render the cell active, all cells were charged at 0.23 A for 13 h before regular cycle testing. Two test methods were employed: the standard cycle testing and the ES driving pattern cycle testing. Standard cycle testing used 0.8 A discharge current to 1.75 V cell cut-off voltage and a 0.4 A charge current to 120% of the previous discharge capacity. In addition, an open circuit period of 30 min was implemented at the end of each half-cycle. Cycling continued until cell capacities have dropped and remained below 80% of the initial capacity. The ES driving pattern in Fig. 1b entailed the use of the Chinese National Standard-D3029 (CNS-D3029) driving schedule in Fig. 1a as negotiated by an Improved Sanyang Dio ES [1]. This schedule's average velocity was 22.5 km h^{-1}, with the scooter traveling $\sim$0.7 km during one cycle of the schedule. The ES driving pattern cycle test was composed of 112 s in length, six steps and four power levels. In the ES driving cycle testing, cells were cycled under the following procedure: a constant power discharge according to each power step on the schedule was repeated until the cell voltage fell below 1.75 V cell cut-off voltage and a 0.4 A charge current to 130% of the previous discharge capacity. Finally, an open circuit period of 30 min was implemented at the end of each half-cycle.

2.3. Analysis of positive plate material

The positive material's physicochemical properties, including the phase composition, morphology and specific area (porosity), were obtained by X-ray powder diffraction (XRD), scanning electron microscopy (SEM), and Brunauer–Emmet–Teller (BET)-N_2 adsorption methods. All analytical samples taken from the plates were treated using the following steps [2]:

1. Wash with distilled water (to remove acid);
2. Wash with absolute ethanol (to removed water) and dry in a desiccator; and
3. After drying, a portion of each sample was gently ground using a pestle and mortar.

3. Results and discussion

3.1. Analyses of plate composition and morphology

The behavior of the positive plates markedly influences the deep-discharge service of VRLA batteries, especially in ES applications. In our earlier paper [1], we investigated how curing temperature affected the positive plate material composition and morphology, and the performance of VRLA cells for ES applications. The higher curing temperature (>65°C), formed 4BS-rich positive plate materials, which have stronger mechanical strength and enhance the

Table 1
Comparison of phase compositions and BET-specific surface areas of cured and formed active material

Sample	Composition weight percent ($\pm$4%)						BET-specific surface area ($m^2\ g^{-1}$)
	α-PbO	4BS ($4PbO \cdot PbSO_4$)	HC ($2PbCO_3 \cdot Pb(OH)$)	α-PbO_2	β-PbO_2	$PbSO_4$	
A group (0 M Na_2SO_4)							
After 85°C curing	34.7	61.5	3.8				0.38
After formation				41.8	53.4	4.8	2.78
B group (0.01 M Na_2SO_4)							
After 85°C curing	31.4	64.3	4.3				0.48
After formation				42.3	52.3	5.4	3.34
C group (0.05 M Na_2SO_4)							
After 85°C curing	27.4	60.5	4.1				0.51
After formation				45.1	49.3	5.6	3.68
D group (0.5 M Na_2SO_4)							
After 85°C curing	30.1	66.2	3.7				0.45
After formation				44.2	50.6	5.2	3.37
E group (1 M Na_2SO_4)							
After 85°C curing	32.9	62.8	4.3				0.41
After formation				41.3	53.8	4.9	3.20
F group (2 M Na_2SO_4)							
After 85°C curing	28.6	67.5	3.9				0.40
After formation				40.8	54.1	5.1	3.08

cycle life for ES applications. However, 4BS crystallizes into large prismatic needles, leading to a lower capacity because of the smaller surface area. The additive Na_2SO_4 in the positive electrode material can reduce the 4BS crystal size, which has a larger surface area and increase the cell capacity. This work aimed to determine the effects of the different amounts of Na_2SO_4 additive on the performance of the positive electrode at higher curing temperatures ($>85°C$). Various amounts of Na_2SO_4 additive, from 0.01 to 2 M Na_2SO_4, were studied. According to the amount of Na_2SO_4 additive, six proportion groups, A, B, C, D, E and F were studied representing the Na_2SO_4 concentrations at 0 (blank, without additive), 0.01, 0.05, 0.5, 1, and 2 M, respectively. In order to increase the reliability of the experimental results, a total of five cells of each group type were fabricated and subjected to performance tests. Table 1 presents the physicochemical and XRD analyses of all sulfates in all group plates after formation and curing at 85°C. According to the results, the major cured plate constituent is 4BS and α-PbO together with some HC (Hydrocerussite; $2PbCO_3 \cdot Pb(OH)_2$). During formation, the phase composition converts into α-PbO_2 and β-PbO_2 with some $PbSO_4$. The plate's chemical composition is independent of the amount of Na_2SO_4 additive in the positive electrodes. Similar to our former results [1], the plate's chemical composition relies heavily only on the temperature conditions. Table 1 also shows that group A without any Na_2SO_4 additive has a smaller specific surface area. This result indicates that the additive Na_2SO_4 in the cured plates can reduce the 4BS crystal size and produce a smaller surface area. The groups B and C contained 0.01–0.05 M Na_2SO_4 additive, producing a larger specific surface area. Similar to the results with the cured plates, the positive electrodes with Na_2SO_4 additive exhibited a larger surface area after plate formation. The smaller 4BS crystal size in the cured plates caused a smaller α-PbO_2 and β-PbO_2 crystal size in the formed plates. Fig. 2 shows the XRD patterns for the samples

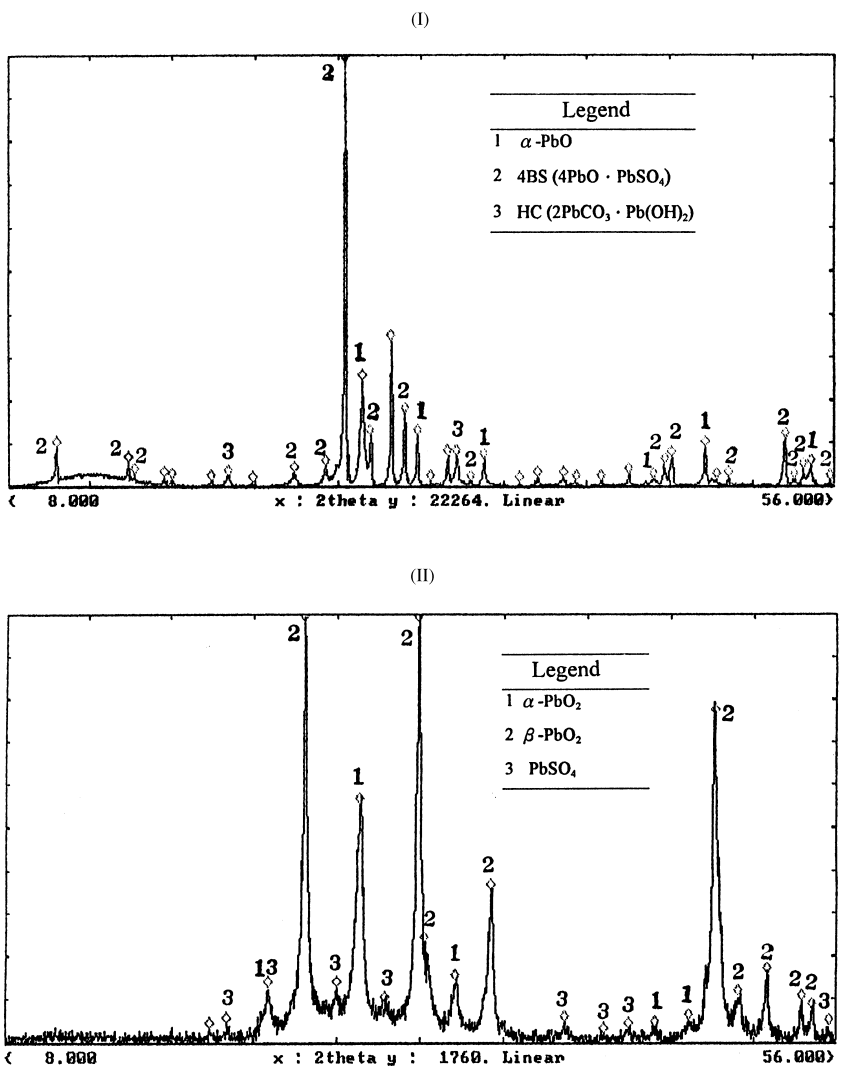

Fig. 2. XRD patterns for samples from group B cells. (I) Cured plates. (II) Formed plates.

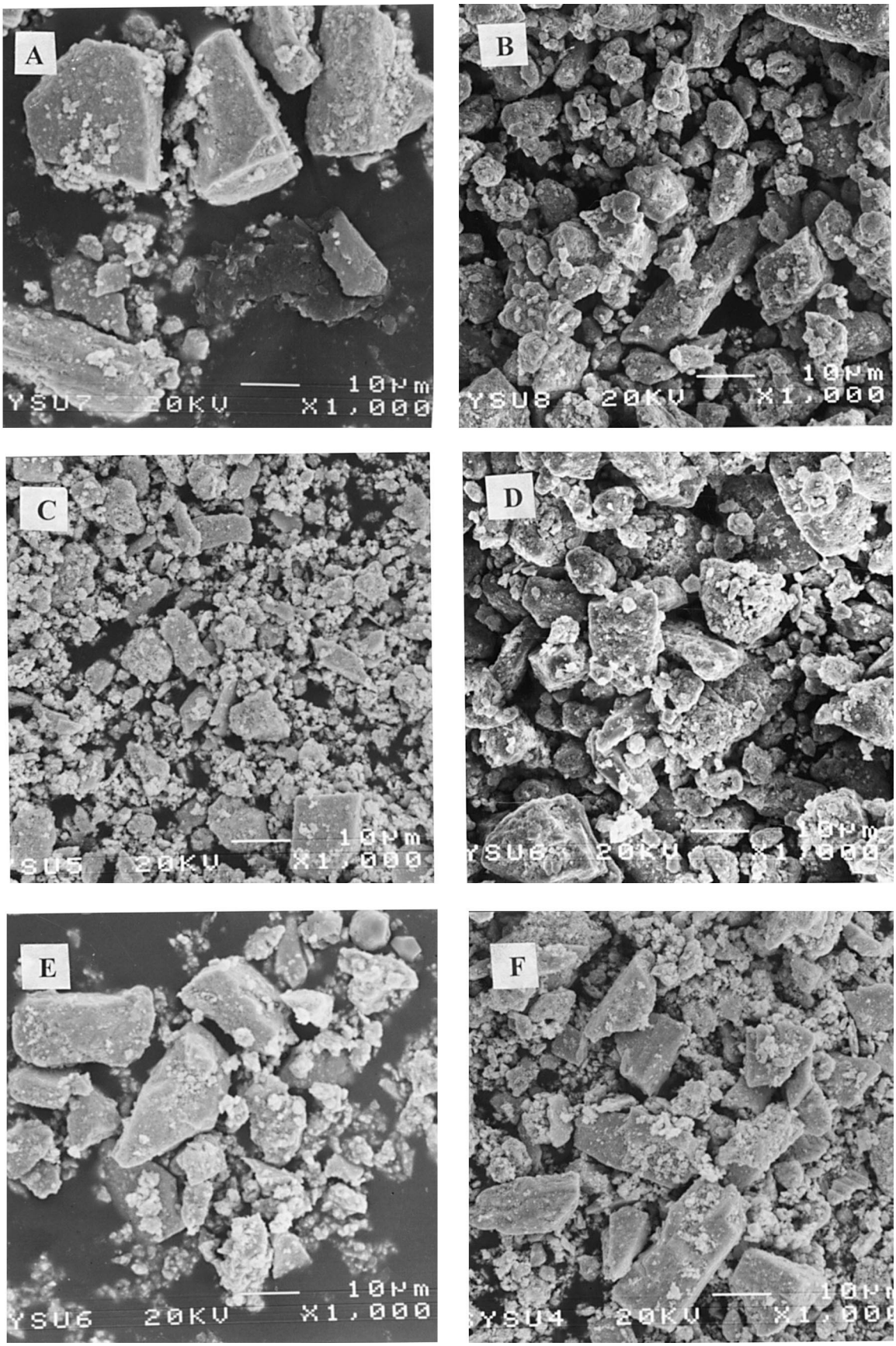

Fig. 3. Scanning electron micrographs of cured crystals in groups A to F cells with different amounts of Na_2SO_4 additive.

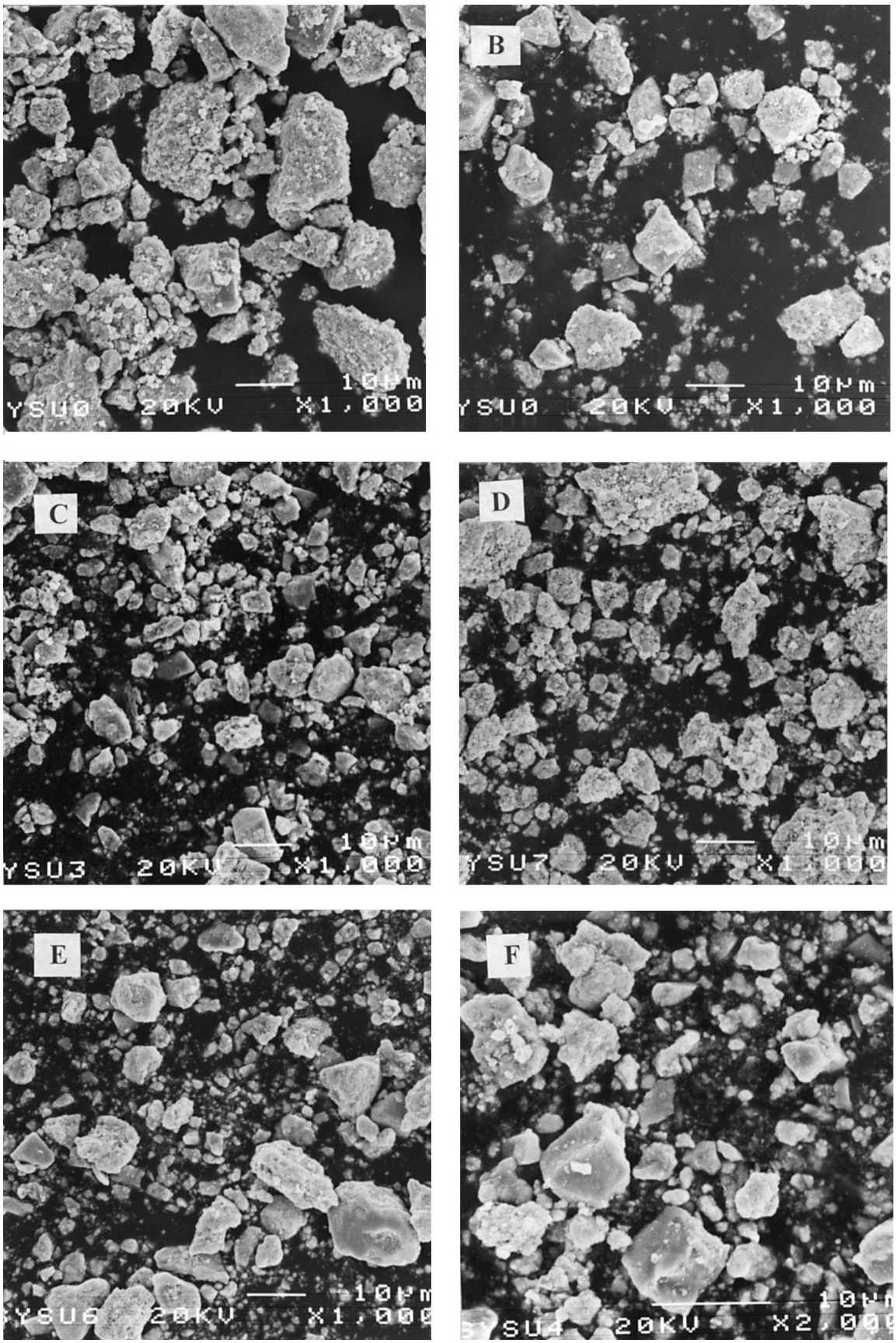

Fig. 4. Scanning electron micrographs of formed crystals in groups A to F cells with different amounts of Na_2SO_4 additive.

Table 2
Cycle-life performance data for representative groups of 4.0 A h VRLA cells

Sample	Cycle number	Initial capacity (A h)	Capacity loss/cycle (%)	Average capacity/cycle (A h)
A (0 M Na_2SO_4)	193	3.92	0.111	3.71
B (0.01 M Na_2SO_4)	210	4.05	0.107	3.87
C (0.05 M Na_2SO_4)	196	4.08	0.114	3.86
D (0.5 M Na_2SO_4)	208	4.01	0.104	3.83
E (1 M Na_2SO_4)	183	3.97	0.122	3.75
F (2 M Na_2SO_4)	198	3.94	0.114	3.69

from group B in cured and formed plates, respectively. The results demonstrate that the major constituent is 4BS and α-PbO together with some HC in the cured plate and α-PbO_2 and β-PbO_2 with some $PbSO_4$ in the formed plate. Fig. 3 presents scanning electron micrographs of cured crystals in the groups A–F samples at different amounts of Na_2SO_4 additive. The cured paste consists of larger 4BS crystals together with smaller α-PbO crystals. The 4BS crystals have an elongated prismatic form and each grain consists of many sub-grains. The crystal size distributes from 1 to 20 μm. The 4BS crystals exhibit a smaller size in the cured plate with Na_2SO_4 additives. However, increasing amounts of Na_2SO_4 additive to the positive electrode do not continue to decrease the crystal size. The results show that groups B and C exhibit the smallest crystal size. Fig. 4 shows scanning electron micrographs of formed crystals in the A–F group samples at different amounts of Na_2SO_4 additive. Similar to the results with the BET-specific surface area analysis, the smaller 4BS crystal size decreases in the formed plates. Generally, the 4BS crystal was produced using two steps. In the first mixing step, 3BS ($3PbO \cdot PbSO_4 \cdot H_2O$) is formed in the mixing of the leady oxide with H_2O and H_2SO_4 solution. 4BS crystal is formed at a higher temperature and a relative humidity from 3BS and α-PbO during the second curing step [2,4,11,12]. The smaller 4BS crystal size produced can be attributed to adding Na_2SO_4 additive, which increases the amount of SO_4^{-2} ions and results in a larger amount of initial nucleus formed in the first mixing step. The larger amount of nucleus reduces the 4BS crystal size during the 4BS crystal growth in the second curing step.

3.2. Cell standard cycle-life performance

This work also attempted to determine the effects of different amounts of Na_2SO_4 additive on cells' performance. Six groups of cells with various amounts of Na_2SO_4 additive were subjected to two test methods: the standard cycle test and the ES driving pattern cycle test. In this study, five cells in each group were tested with the average performance based on the results exhibited by five cells. Six groups of cells were subjected to standard cycle-life testing: group A cells (without Na_2SO_4 additive, as a control test for comparison purposes) and groups B–F

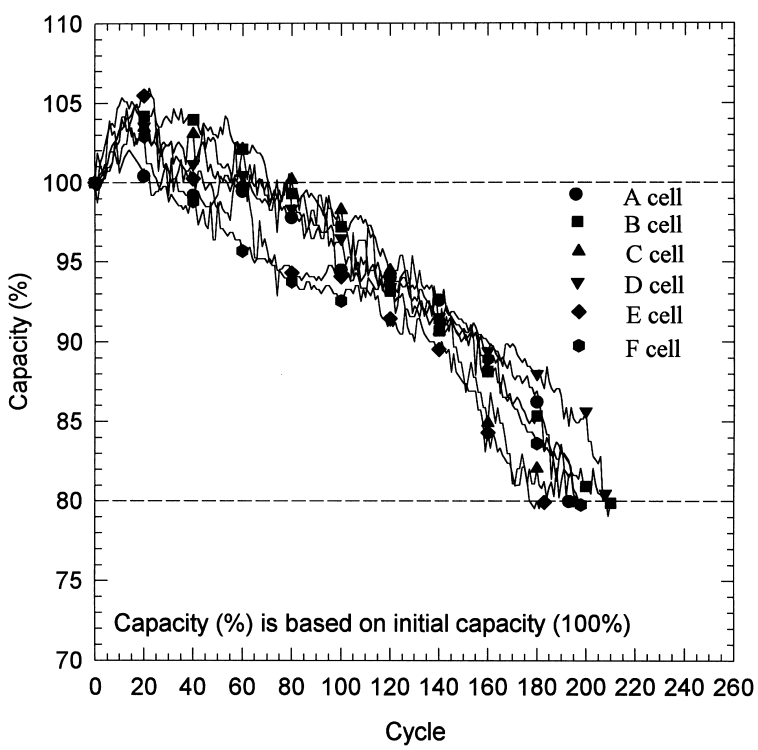

Fig. 5. Capacity vs. cycle number for groups A to F cells.

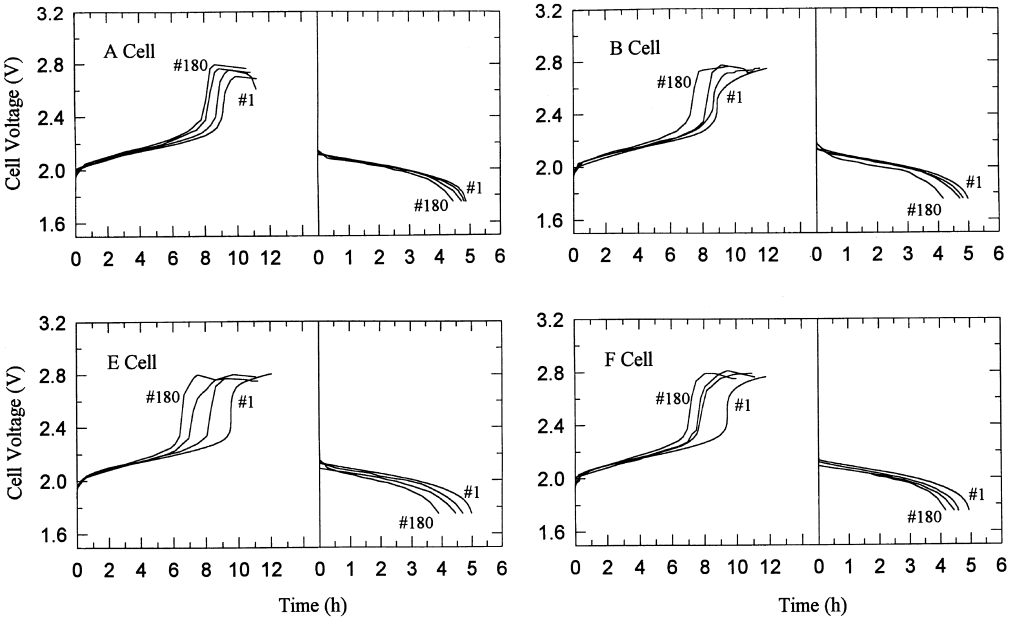

Fig. 6. Cell voltage at different cycles for cells A, B, E and F. Potential vs. time curves are identified for first cycle and 180th cycle. The curves for intermediate cycles (nos. 80, 120) are shown, but not identified.

cells (with various amounts of Na_2SO_4 additive) listed in Table 2. Group A cells were used as the control for cell testing in all of the cell groups. The cell capacity data shown in Table 2 are based on initial cell capacity. The table includes the values of the capacity loss rate and the average delivered capacity per cycle, both based on the cell performance before its capacity dropped to 80% of the initial capacity. The capacity loss rate, expressed as percentage per cycle, is based on the initial cell capacity and can be estimated using:

$$Y = \left(1 - C_+^{1/n}\right) \times 100,$$

where n denotes the total cycle number, C_+ represents the terminal fractional capacity (based on the initial cell capacity), and Y is the average fractional capacity loss for each cycle. According to Table 2, the cycle life of all cells had about 200 cycles for all standard cycles. The similar cycle life in all groups of cells can be attributed to the same curing temperature at 85°C for the positive electrodes. However, cells with Na_2SO_4 additive in the positive electrode exhibited a higher average capacity per cycle than the standard cells without Na_2SO_4 additive. The initial capacity and average capacity could be increased up to 4%. The difference in cell capacity can be attributed to the specific surface area of the crystals in the positive electrode. The positive electrodes with Na_2SO_4 additive exhibited a smaller 4BS crystal with a larger specific surface area and higher initial capacity and average capacity per cycle. This result also demonstrated that increasing the amount of Na_2SO_4 additive in the positive electrode will not substantially increase the initial capacity. Groups B and C with 0.01–0.05 M Na_2SO_4 additive had a higher initial capacity and average capacity per cycle. All of the cells had a capacity loss per cycle of about 0.11%. Fig. 5 shows a plot of capacity vs. cycle number for all cell groups. The capacity of all cells reached their maximum values (~105%) after roughly 15 cycles, remaining above 80% up to 200 cycles at 100% depth-of-discharge (DOD). Adding the Na_2SO_4 additive to the positive electrode produced a higher capacity, but the cycle life was the similar. Fig. 6 depicts the cell voltage at various cycles for group cells A, B, and C. As the data reveal, all cells exhibited the expected charge and discharge curves shape.

3.3. Cell ES driving pattern cycle-life performance

Six group cells were subjected to the ES driving pattern cycle testing to assess the effect of various amounts of Na_2SO_4 additive in the positive electrode listed as in Table 3. The cell capacity data shown in Table 3 are based on the cell initial capacity. Table 3 confirms that cells with

Table 3
Cycle-life performance data for representative groups of 4.0 A h VRLA cells under the ES driving pattern

Sample	Cycle number	Initial capacity (A h)	Capacity loss/cycle (%)	Average capacity/cycle (A h)
A (0 M Na_2SO_4)	95	3.25	0.235	2.93
B (0.01 M Na_2SO_4)	98	3.45	0.229	3.19
C (0.05 M Na_2SO_4)	96	3.47	0.233	3.20
D (0.5 M Na_2SO_4)	99	3.38	0.223	3.15
E (1 M Na_2SO_4)	96	3.29	0.232	3.03
F (2 M Na_2SO_4)	94	3.30	0.237	3.02

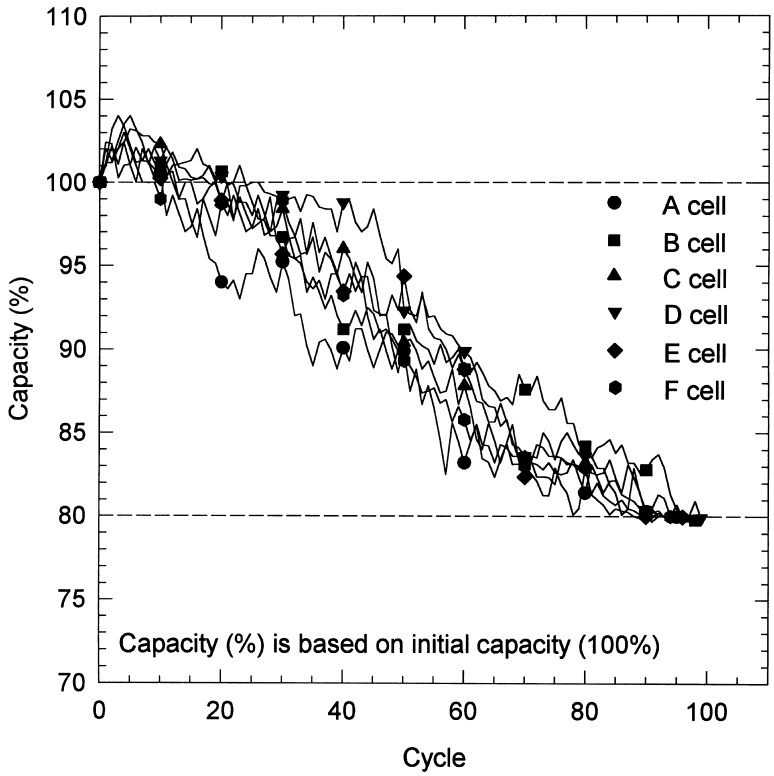

Fig. 7. Capacity vs. cycle number for groups A to F cells under ES driving pattern.

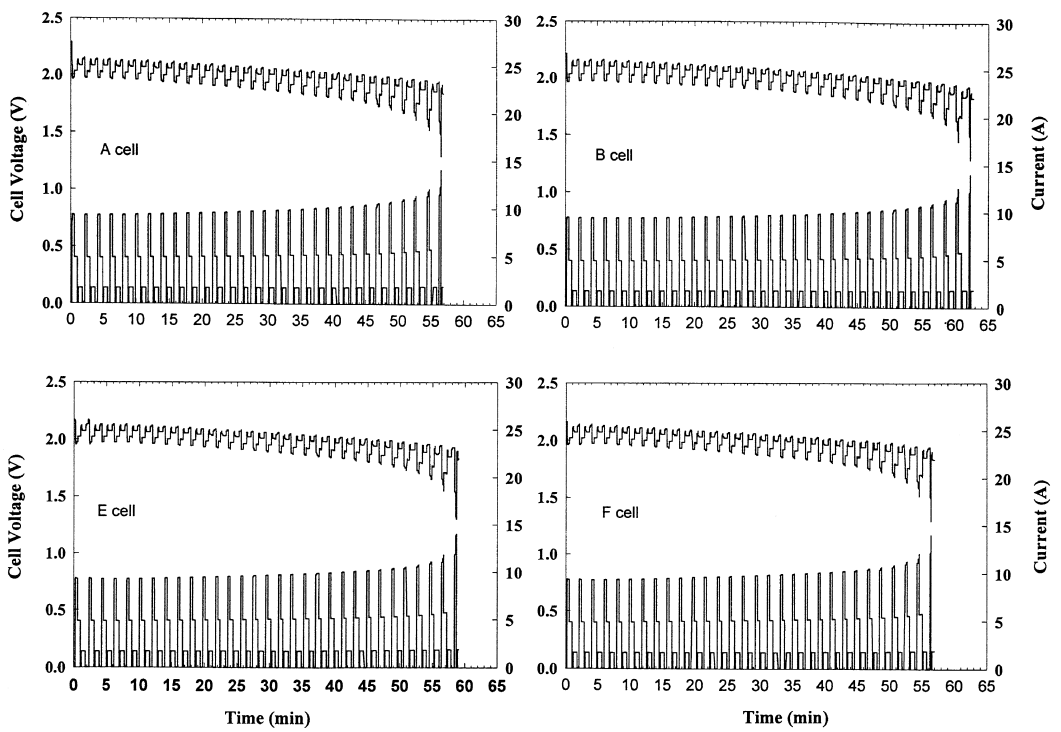

Fig. 8. Cell, voltage and discharge current vs. time during first cycle for cells A, B, E and F under ES driving pattern.

Na_2SO_4 additive in the positive plates have a higher initial capacity and average capacity per cycle. Groups B and C with 0.01–0.05 M Na_2SO_4 additive had a higher initial capacity and average capacity per cycle. Similar results can be found in Table 2. However, the initial capacity and average capacity could be increased up to 8% in the ES driving pattern cycle testing. The capacity loss per cycle, about 0.23% in the ES driving pattern cycle testing, was greater than that in the standard cycle testing. Fig. 7 presents capacity vs. cycle number for all group cells A–F under ES driving pattern in Fig. 1b. Similar to Fig. 5, the capacity of all cells reached their maximum values (~ 104%) after about five cycles, and remained above 80% for up to 95 cycles. Various amounts of added Na_2SO_4 produced similar cycle life, but yielded a higher initial capacity and average capacity per cycle. Fig. 8 depicts the cell voltage and discharge current vs. time during the first cycle for A, B, and C group cells. In the peak load (60 W kg^{-1}) period, the discharge current reached the highest value while the cell voltage fell to its lowest one. Moreover, with each successive sub-cycle, the average voltage followed a downward trend and the discharge current increased. All of the cells completed about 32 sub-cycles before the terminal voltage fell to the cut-off value. The most useful energy density per cell was calculated to be around 25 W h kg^{-1} and the range was about 23 km.

4. Conclusions

The performance of a sealed lead-acid battery is determined by the behavior of the positive electrode. During positive electrode production, a curing process operated at high temperature and humidity will result in 4BS active material that crystallizes as large prismatic needles. Electrodes made with a large amount of 4BS will have less initial capacity because of the lower surface area, but have a longer cycle life. This study investigated the effects of Na_2SO_4 additive in the positive electrode on the performance of VRLA cells. Based on the results presented herein, we can conclude the following.

(1) The XRD analyses showed that the major constituent of the additive Na_2SO_4 in the cured plates is 4BS and α-PbO together with some HC and α-PbO_2 and β-PbO_2 with some $PbSO_4$ in the formed plates. The plate's chemical composition is independent of the amount of Na_2SO_4 additive in the positive electrodes. Plate composition relies heavily on the cure temperature conditions.

(2) The additive Na_2SO_4 in the cured plates can reduce the 4BS crystal size, which produces a smaller α-PbO_2 and β-PbO_2 crystal size in the formed plates and has a larger surface area. Increasing the amount of Na_2SO_4 additive to the positive electrode will not decrease the crystal size appreciably. The Na_2SO_4 additive containing 0.01–0.05 M produces the smallest crystal size and largest specific surface area.

(3) The positive electrodes with Na_2SO_4 additive have smaller 4BS crystals, which have a larger specific surface area and cause higher initial capacity and average capacity per cycle for both testing methods: the standard cycle testing and the ES driving pattern cycle testing. The initial and average capacities can be increased up to 4% in the standard cycle testing and up to 8% in the ES driving pattern cycle testing.

(4) Higher curing temperature for positive plate materials enhances the cycle life for deep-discharge applications in sealed lead-acid batteries. Na_2SO_4 additive in positive plates can increase the cell's capacity while producing a longer cycle life at high cure temperatures. Next, our future research will continue to focus on how to increase positive plate utilization at higher cure temperatures.

Acknowledgements

This author would like to thank the ROC National Science Council for financially supporting this work under contract no. NSC-86-2214-E-214-002. Ztong Yee Battery and Success Battery (in Taiwan) provided several electrodes and cell parts. The author thanks Ztong Yee Battery and Success Battery for proving these useful materials.

References

[1] J.-S. Chen, L.F. Wang, J. Power Sources 70 (1998) 269–275.
[2] D.A.J. Rand, R.J. Hill, M. McDonagh, J. Power Sources 31 (1990) 203–215.
[3] J.K. Vilhunen, S. Hornytzkyj, J. Power Sources 39 (1992) 59–65.
[4] V. Iliev, D. Pavlov, J. Appl. Electrochem. 9 (1979) 555–562.
[5] B. Culpin, J. Power Sources 25 (1989) 305–311.
[6] D.A.J. Rand, J. Power Sources 64 (1997) 157–174.
[7] S.V. Baker, P.T. Moseley, A.D. Turner, J. Power Sources 27 (1989) 127–143.
[8] K.R. Bullock, B.K. Mahato, W.J. Wruck, J. Electrochem. Soc. 138 (1991) 3545.
[9] T. Rogachev, D. Pavlov, J. Power Sources 64 (1997) 51–56.
[10] B. Vyas, R.E. Landwehrel, M.N. Thomas, Proceeding of the symposium on advanced in batteries, Proc. Electrochem. Soc., 94-2, p. 258.
[11] L. Zerroual, N. Chelali, F. Tedjar, J. Power Sources 51 (1994) 425–431.
[12] G.L. Corino, R.J. Hill, A.M. Jessel, D.A.J. Rand, J.A. Wunderlich, J. Power Sources 16 (1985) 141–168.